

1 **Benefit of China's emission reduction in nitrogen oxides to**
2 **natural ecosystems in East Asia: In aspect of critical load**
3 **exceedance**

4
5 **Danni Xie¹, Bin Zhao², Shuxiao Wang^{1,3}, Lei Duan^{1,3,*}**

6 ¹ State Key Laboratory of Environmental Simulation and Pollution Control, School of Environment,
7 Tsinghua University, Beijing 100084, PR China.

8 ² Joint Institute for Regional Earth System Science and Engineering and Department of Atmospheric
9 and Oceanic Sciences, University of California, Los Angeles, California 90095, USA.

10 ³ Collaborative Innovation Centre for Regional Environmental Quality, Tsinghua University, Beijing,
11 100084, PR China.

12 *Corresponding Authors: lduan@tsinghua.edu.cn

13
14 **ABSTRACT:** The emission of nitrogen oxides (NO_x) in China decreased by 17% from
15 2011 to 2017 (without a significant decrease in NH₃ emission), resulting in the
16 declination of nitrogen (N) deposition in East Asia. Empirical N critical load
17 exceedance was used to assess the benefit of the NO_x emission reduction in China to
18 natural ecosystems in East Asia. Empirical N critical loads for major forest and
19 grassland types in East Asia were assigned on the bases of field manipulation
20 experiments for N effects. Results demonstrated that empirical N critical loads in East
21 Asia were far greater than those in Europe and America. The critical load map based

22 on the minimum of the critical load range of each vegetation type showed that empirical
23 critical loads were generally lower in the Tibetan Plateau and some parts of northeastern
24 China ($\leq 5 \text{ kgN}\cdot\text{ha}^{-1}\cdot\text{a}^{-1}$), and higher in northern and southern China ($\geq 20 \text{ kgN}\cdot\text{ha}^{-1}\cdot\text{a}^{-1}$). Empirical critical loads were also low in some parts of central and northern Japan (\leq
25 $5 \text{ kgN}\cdot\text{ha}^{-1}\cdot\text{a}^{-1}$) and the south of Korean Peninsula ($5\sim 10 \text{ kgN}\cdot\text{ha}^{-1}\cdot\text{a}^{-1}$). As a result of
26 NO_x emission reduction in China, N deposition in East Asia decreased significantly
27 from 2010 to 2015. Consequently, the area and total amount of critical load exceedance
28 in East Asia declined by 5.22% and 4.80% respectively, implying great benefit to
29 natural ecosystems.

31 **KEYWORDS:** NO_3^- deposition, natural and semi-natural ecosystems, N critical
32 threshold, positive response

33

34 **1 Introduction**

35 In the past two decades, the economy in East Asia has developed rapidly, resulting
36 in rapid growth in NO_x emissions (Mijling et al., 2013), and the highest nitrogen (N)
37 deposition in the world (Vet et al., 2014), with modeled values higher than $20 \text{ kgN}\cdot\text{ha}^{-1}\cdot\text{a}^{-1}$
38 in most of areas in Eastern China, the Korean Peninsula, and Japan (Ban et al.,
39 2016; Duan et al., 2016; Endo et al., 2011; Galloway et al., 2005; Schwede et al., 2018;
40 Vet et al., 2014). Both modeling and monitoring results showed that N deposition in
41 Eastern China was commonly higher than $40 \text{ kgN}\cdot\text{ha}^{-1}\cdot\text{a}^{-1}$ (Chen and Mulder, 2007;
42 Fan et al., 2007a; Larssen et al., 2006; Zhao et al., 2009a; Zhu et al., 2015), with the

43 highest values exceeding 60 kg N ha⁻¹ yr⁻¹ (Xu et al., 2015; Zhao et al., 2017a). That
44 level was well above the peak N deposition value currently observed in Europe and
45 North American (Du, 2016; Fagerli and Aas, 2008; Theobald et al., 2019), and
46 exceeded the critical loads for most of natural ecosystems in Europe and America
47 (Bouwman et al., 2012; de Vries et al., 2015). High N deposition may result in N
48 saturation in ecosystem (Bobbink et al., 2010), causing negative effects, such as
49 eutrophication and acidification of soil and water (Bowman et al., 2008; Hogberg et al.,
50 2006), emission of N₂O (Xie et al., 2018; Zhu et al., 2013), imbalance of plant nutrients
51 (Liu et al., 2013a), and reduction in plant biomass and biodiversity (Aber et al., 1995;
52 Clark and Tilman, 2008; Du and Fang, 2014; Gilliam, 2006; Jiang et al., 2017; Kreutzer
53 et al., 2009; Silvertown et al., 2006; Tian et al., 2017a). Numerous N fertilization
54 experiments carried out since the early 2000s in East Asia, both in forests and
55 grasslands (Table 1), have shown the negative effects of elevated N deposition on
56 natural and semi-natural ecosystems.

57 Critical load of N is defined as “a quantitative estimate of an exposure to one or more
58 pollutants below which significant harmful effects on specified sensitive elements of
59 the environment do not occur according to present knowledge” (Nilsson and Grennfelt,
60 1988). According to the concept, when N deposition exceeds its critical load, the
61 ecosystem is expected to be damaged. Critical load has been widely used as the
62 guideline for the emission abatement in Europe and American (CLRTAP, 2017;
63 Hettelingh et al., 1995, 2009; McNulty et al., 2013; Posch et al., 2001), as well as in

64 China (Hao et al., 2001).

65 Critical loads of N can be estimated by empirical approach (Bobbink et al., 2010),
66 steady-state mass balance (SSMB; UBA, 2004), and dynamic modeling (de Vries et al.,
67 2010). In comparison with SSMB and dynamic modeling, which are both based mass
68 balance calculation and need adequate and detailed data (even much more by the latter)
69 for input parameters or model calibration, empirical approach, based on observed
70 responses of certain ecosystem to N deposition, has been more widely applied in
71 regional study and mapping of critical loads, especially in the United States (Clark et
72 al., 2018; Geiser et al., 2019; Lynch et al., 2013; Pardo et al., 2011), Canada (NEG-ECP,
73 2001), and Europe (Bobbink et al., 2010; CLRTAP, 2017). Similarly, newer findings on
74 the various responses of forests and grasslands to N deposition by the manipulation
75 experiments carried out in East Asia can be used to assign the empirical N critical loads.
76 Although critical loads of nitrogen were calculated through SSMB method several
77 years ago in East Asia (Duan et al., 2001; Park and Bashkin, 2001; Posch et al., 2014),
78 the empirical N critical loads and relative response data can used for testing or
79 confirmation of the SSMB results.

80 The NO_x emissions in China accounted for about 81.7% of the total emissions in
81 East Asia in 2006, with only 9.4% and 5.1% from Japan and South Korea (Zhang et al.,
82 2009). Due to very high NO_x emission in China, long-range transport of the nitrogen-
83 content pollutants occurred from the Asian continent to Japan and South Korea (Morino
84 et al., 2011). During 2000-2008, the total NO_x emissions increased by 54% in East Asia,

85 mainly from China (Kurokawa et al., 2013). However, the NO_x emissions in China
86 started to decrease after China began to perform the National NO_x Total Emission
87 Control in 2011 (MEP, 2011). Until 2017, the national NO_x emissions in China had
88 decreased by about 17% since 2011 (Zheng et al., 2018). Although the main impetus
89 for the Chinese government in reducing NO_x emissions was to improve urban ambient
90 air quality (especially, to reduce PM_{2.5} concentrations; China State Council, 2013; Zhao
91 et al., 2013), the NO_x emission abatement in China also led to reduction in N deposition
92 (mainly nitrate deposition), not only in China, but also in Korea and Japan (EANET,
93 2017). However, it is unclear whether and how much the reduction in N deposition will
94 mitigate the impact on natural ecosystems in East Asia. Therefore, the objective of this
95 study is: (1) to assign empirical N critical loads to major vegetation types in East Asia,
96 (2) to evaluate the risk of N deposition impact on natural ecosystems based on the
97 critical load exceedance of N deposition, and (3) to estimate the benefit of NO_x
98 emission abatement in China during 2010-2015 (the first five years of abatement) by
99 comparing the area of critical load exceedance in East Asia between 2010 and 2015.
100 These results may serve as the first environmental impact assessment of N deposition
101 in East Asia, and may support the future development of N emission abatement policy.

102 **2. Materials and Methods**

103 2.1 Review of N fertilizing experiments and critical load evaluation

104 Empirical N critical loads refer to the level of N deposition where detrimental
105 ecological effects occur (Bobbink et al., 2015; Clark et al., 2018). They are based

106 entirely on observable changes in the structure and function of ecosystems, which can
107 connect N deposition to plant and soil responses (Bobbink et al., 2011; Tipping et al.,
108 2013). Field N fertilization experiments on major forest and grassland types have been
109 widely implemented in East Asia since 2000s (as listed in Table 1, and Figure 1 showing
110 the locations). Liu et al. (2011) and Duan et al. (2014) reviewed the measured chemical
111 and biological changes of grasslands and forests responding to different N input, from
112 published literature and data sets on N fertilization experiments in China. In this study,
113 we updated the summary by adding newer results after 2010 in China and some results
114 from other countries in East Asia. Due to the very lack of long-term N addition
115 experiments in South Korea, North Korea, and southern Japan, critical loads for their
116 ecosystems were assigned according to similar ecosystems in China (as listed in
117 Supplementary Table S1). Various changes in both ecosystem structure involving
118 mycorrhizal fungi (changes in community structure, declines in species richness and so
119 on), herbaceous vegetation and shrubs (changes in foliar nitrogen, reductions in
120 abundance, and so on), and ecosystem functions, such as NO_3^- leaching, increased N_2O
121 emission, and decreased tree growth, were considered for determining empirical critical
122 loads.

123 As in similar experiments being done in Europe and North American, several study
124 sites were located in forest and on grassland, and added with nitrogen fertilizers, mainly
125 using nitrate, ammonium (including urea) or both, by a series of doses. The field
126 experiments we reviewed lasted at least one year, and some of them had implemented

127 for more than five years and were ongoing (Du et al., 2013; Fang et al., 2014; Huang et
128 al., 2015; Lin et al., 2007; Lu et al., 2007; Wan et al., 2008). Since there were quite
129 insufficient studies on N effects in East Asia, all of them, with both low (i.e. close to
130 ambient N deposition) and high doses of fertilizer addition, were included in this review.
131 Each studied ecosystem was assigned a critical load range, the upper limit was the
132 lowest input level at which the response occurred, and the lower limit was the highest
133 input level without any significant impact (Lin et al., 2007). It is important to note that
134 the nitrogen input should be the sum of fertilizer dose and atmospheric N deposition.
135 For a given vegetation type when several critical load ranges were obtained from
136 different studies (Table 1), a critical load range was recommended for safety: from the
137 minimum of the lower limits of all critical load ranges, to the minimum of the upper
138 limits. The critical load map was then plotted (ArcMap 10.2, ESRI Company, Redlands,
139 California, USA) according to the distribution of major vegetation types, the minimums
140 of whose critical load ranges were used for conservative reason and protecting more
141 ecosystems (Figure 2). For comparison, the medians of the critical load ranges were
142 also applied and the map was shown in Supplementary Figure S1. In addition, final
143 empirical critical loads used in empirical critical load map were shown in Table S2.

144 2.2 Nitrogen deposition modeling and critical load exceedance calculation

145 The N deposition (the sum of dry and wet deposition) in East Asia was modeled by
146 the Community Multi-scale Air Quality model with the two-dimensional Volatility
147 Basis Set (CMAQ/2D-VBS) (Zhao et al., 2016). The anthropogenic emission inventory

148 in China during 2010-2015 was developed by Tsinghua University (Zhao et al., 2013,
149 2017b, 2018; Wang et al., 2014). The emissions in countries other than China were
150 obtained from the MIX emission inventory for the year 2010 (Li et al., 2017), which
151 was the latest year available. We calculated biogenic VOC emissions using the Model
152 of Emissions of Gases and Aerosols from Nature (MEGAN; Guenther et al., 2006). The
153 modeling domain, with a 36 km×36 km grid resolution, covers East Asia and some
154 surrounding regions. The meteorological fields used to drive the CMAQ/2D-VBS
155 model was generated by the Weather Research and Forecasting Model (WRF, version
156 3.7). The other model configurations, such as the vertical resolution, physical and
157 chemical schemes, boundary and initial conditions of CMAQ/2D-VBS and WRF, and
158 the mapping of anthropogenic emissions to model grids were the same as Zhao et al.
159 (2018). We chose the whole year of 2010 and 2015 as our simulation periods. We had
160 evaluated the meteorological and chemical simulations against surface and satellite
161 observations, and showed a reasonably good agreement (Zhao et al., 2018). The
162 uncertainty (coefficients of variation) of wet deposition modeling was about -35% for
163 N, on average (Zhao et al., 2009a). The modeling results were then interpolated to grids
164 of 0.1 degree by 0.1 degree (ArcMap 10.2, ESRI Company, Redlands, California, USA).
165 Critical loads were also allocated to the grids of 0.1 degree by 0.1 degree. The
166 difference between the N deposition and critical load of each grid resulted in the critical
167 load exceedance map of East Asia.

168 **3. Results**

169 3.1 Empirical N critical loads for major ecosystems

170 The empirical N critical loads for major forest and grassland types (shown in Table
171 1) varied widely in terms of vegetation types and geographical locations. Among forests,
172 subtropical coniferous plantations had the highest critical load ($170\sim300 \text{ kgN}\cdot\text{ha}^{-1}\cdot\text{a}^{-1}$),
173 and temperate deciduous forests had the lowest ($10\sim30 \text{ kgN}\cdot\text{ha}^{-1}\cdot\text{a}^{-1}$). The critical loads
174 for temperate mixed broad-leaved deciduous and coniferous evergreen forest and
175 subtropical forest (both coniferous and broad-leaved) were $\leq 100 \text{ kgN}\cdot\text{ha}^{-1}\cdot\text{a}^{-1}$. The
176 critical loads of grasslands varied from $\leq 50 \text{ kgN}\cdot\text{ha}^{-1}\cdot\text{a}^{-1}$ for alpine meadow, alpine
177 steppe, temperate grass-forb community, and temperate grass-forb meadow, to $150\sim250$
178 $\text{kgN}\cdot\text{ha}^{-1}\cdot\text{a}^{-1}$ for subtropical and tropical grass - forb community. Other grassland types
179 had critical loads of $50\sim100 \text{ kgN}\cdot\text{ha}^{-1}\cdot\text{a}^{-1}$, including temperate needlegrass arid steppe.

180 3.2 Mapping empirical N critical loads and their exceedance

181 The empirical N critical loads were low on the Tibetan Plateau and in some parts
182 of northeastern China ($\leq 5 \text{ kgN}\cdot\text{ha}^{-1}\cdot\text{a}^{-1}$) (Figure 2). In contrast, the critical loads for
183 subtropical ecosystems in southern China, where high N deposition occurred, were in
184 the range of $30\sim200 \text{ kgN}\cdot\text{ha}^{-1}\cdot\text{a}^{-1}$. The critical loads were also low ($\leq 5 \text{ kgN}\cdot\text{ha}^{-1}\cdot\text{a}^{-1}$) in
185 some parts of central and northern Japan (for Hokkaido deciduous forests and Nihonkai
186 Montane deciduous forests) and in the south of Korean Peninsula (for central Korean
187 deciduous forests and southern Korean evergreen forests). It should be noted that there
188 were no data available for areas where the main plant types are shrubs (in white on the
189 critical load map).

190 Modeling results showed that N deposition in China increased from west to east,
191 which was much higher in the east than in the west, with additional high areas along
192 the southwestern border (Figure 3). In 2010, the higher N deposition was concentrated
193 in southern, eastern, and some parts of northeastern China ($> 20 \text{ kgN}\cdot\text{ha}^{-1}\cdot\text{a}^{-1}$), even
194 higher than $50 \text{ kgN}\cdot\text{ha}^{-1}\cdot\text{a}^{-1}$ in part of southwestern China, while the N deposition in
195 western and some parts of northeastern China was lower ($\leq 5 \text{ kgN}\cdot\text{ha}^{-1}\cdot\text{a}^{-1}$). The N
196 deposition in the Korean peninsula was higher in the north ($20\sim 30 \text{ kgN}\cdot\text{ha}^{-1}\cdot\text{a}^{-1}$) and
197 lower in the south ($10\sim 20 \text{ kgN}\cdot\text{ha}^{-1}\cdot\text{a}^{-1}$). The N deposition in Japan was generally within
198 the range of $10\sim 20 \text{ kgN}\cdot\text{ha}^{-1}\cdot\text{a}^{-1}$, with the lowest in northern Hokkaido ($5\sim 10 \text{ kgN}\cdot\text{ha}^{-1}\cdot\text{a}^{-1}$)
199 and the largest in a small part of central Japan ($20\sim 30 \text{ kgN}\cdot\text{ha}^{-1}\cdot\text{a}^{-1}$). In 2015, the
200 distribution of N deposition in East Asia was similar to that in 2010, with remarkable
201 decrease in all the region except the southwestern border of China (due mainly to
202 increasing transport from South Asia).

203 The difference between nitrogen deposition modeled and the empirical critical loads,
204 led to the critical load exceedance map of East Asia (Figure 4). Empirical N critical
205 loads were exceeded mainly in northeastern, central, and some parts of southern China
206 in 2010, where temperate deciduous forests and temperate grasslands and meadows are
207 the dominant natural vegetation. In general, critical load exceedances of temperate
208 deciduous broad-leaved forests in northeastern and central China were higher than 15
209 $\text{kgN}\cdot\text{ha}^{-1}\cdot\text{a}^{-1}$, and those of temperate grasslands and meadows ranged from $5\sim 15$
210 $\text{kgN}\cdot\text{ha}^{-1}\cdot\text{a}^{-1}$. The main vegetation types with critical load exceedances ranged from $0\sim 5$

211 $\text{kgN}\cdot\text{ha}^{-1}\cdot\text{a}^{-1}$ were temperate grasslands and temperate deciduous broad-leaved forests
212 in some parts of northeastern China. Critical load exceedances also occurred in the
213 southern and some parts of northern Korean peninsula, where Changbai Mountains
214 mixed forests and Central Korean deciduous forests are the dominant natural vegetation.
215 The exceedances of Central Korean deciduous forests in southern Korean peninsula
216 were lower ($\leq 5 \text{ kgN}\cdot\text{ha}^{-1}\cdot\text{a}^{-1}$), while those of Changbai Mountains mixed forests and
217 Central Korean deciduous forests in central Korean peninsula were $5\sim 15 \text{ kgN}\cdot\text{ha}^{-1}\cdot\text{a}^{-1}$.
218 In addition, critical load exceedances occurred in most part of Japan, with lower
219 exceedances of Hokkaido Montane conifer forests and Nihonkai evergreen forests (≤ 5
220 $\text{kgN}\cdot\text{ha}^{-1}\cdot\text{a}^{-1}$) and higher of Hokkaido deciduous forests, Nihonkai Montane deciduous
221 forests, and Taiheiyo evergreen forests ($5\sim 15 \text{ kgN}\cdot\text{ha}^{-1}\cdot\text{a}^{-1}$). In 2015, the distribution of
222 critical load exceedance in China was similar to that in 2010, but the total area and
223 amount of critical load exceedance in China decreased by 5.62% and 4.31%,
224 respectively (Table 2). However, the areas with critical load exceedance of alpine
225 meadows and steppes near northwestern border of China increased due to an increase
226 in N deposition (Figure 3). The total area and amount of critical load exceedance in
227 Japan also decreased by 6.82% and 6.00%, respectively (Table 2). Although the
228 distribution and total area of critical load exceedance in Korean peninsula did not much
229 change in 2015, the total amount of critical load exceedance decreased by 13.5%. In
230 summary, the total area and amount of critical load exceedance in East Asia was
231 estimated to 150 Mha and 12.5 Mt N a^{-1} respectively in 2010, and declined to 142 Mha

232 and 11.9 Mt N a⁻¹ respectively in 2015.

233 **4. Discussions**

234 4.1 Comparison with critical loads in Europe and North America

235 The N demands for different vegetation types differ, as well as the inherent sensitivity
236 of plants, resulting in wide variation of empirical N critical loads for major forest and
237 grassland types (Bobbink et al., 2010; Gao et al., 2014). For forests in East Asia,
238 temperate deciduous forests are more sensitive to increased N input. In contrast,
239 subtropical forests have higher tolerance for N, especially subtropical coniferous forests.
240 For grassland, alpine steppe is the most sensitive to increased N, while temperate
241 needlegrass arid steppe has higher empirical critical loads. These findings are consistent
242 with the results of long-term studies in North America and Europe (Bobbink et al., 2015;
243 Pardo et al., 2011).

244 Empirical N critical loads in East Asia were generally much higher than those in
245 Europe and North America. For example, the critical loads for alpine ecosystems,
246 dessert grassland, and temperate forests in North America were 5~15 kgN·ha⁻¹·a⁻¹, 3~9
247 kgN·ha⁻¹·a⁻¹, and <20 kgN·ha⁻¹·a⁻¹, respectively (Pardo et al., 2011), whereas those in
248 East Asia were 5~55 kgN·ha⁻¹·a⁻¹, 5~105 kgN·ha⁻¹·a⁻¹, and 10~120 kgN·ha⁻¹·a⁻¹,
249 respectively. The empirical N critical loads ranged 3~30 kgN·ha⁻¹·a⁻¹ in Europe, mostly
250 based on data for temperate ecosystems (Bobbink et al., 2015). In particular, empirical
251 N critical loads for coniferous and broadleaved forests were 5~15 kgN·ha⁻¹·a⁻¹ and
252 10~20 kgN·ha⁻¹·a⁻¹, respectively, in Europe (Bobbink et al., 2015), while 30~80

253 $\text{kgN}\cdot\text{ha}^{-1}\cdot\text{a}^{-1}$ and $70\sim 150\text{ kgN}\cdot\text{ha}^{-1}\cdot\text{a}^{-1}$ in China.

254 There may be several reasons for the much higher critical loads in East Asia. Warm
255 and humid subtropical ecosystems have a fast N cycling and thus loss by leaching or
256 N_2O emission (Huang et al., 2015; Xie et al., 2018a, b). In addition, the background of
257 environmental factors such as historical acidification, land use types, starting soil pH,
258 and species abundance, is important for quantifying the thresholds (Bobbink et al., 2010;
259 de Vires et al., 2010). East Asia, especially China has higher planting and harvesting
260 rate than in Europe and North America (Hu et al., 2019), causing higher N demand for
261 forest and grassland ecosystems. Sometimes it is difficult to distinguish whether the
262 negative effect is caused by nitrogen deposition or other human activities, such as soil
263 degradation by over-grazing, and soil acidification by simultaneously high sulfur
264 deposition (Bobbink and Roelofs, 1995; Bobbink et al., 2010). For example, the results
265 of field experiment of N fertilization at Tieshanping in southwestern China showed that
266 the change of ground vegetation diversity in subtropical coniferous forests was mostly
267 attributed to soil acidification due to the high acid deposition in southern China, while
268 the effect of nitrogen saturation might be neglected or underestimated (Huang et al.,
269 2015).

270 Historically high N deposition may be another important reason of high empirical
271 critical loads. Due to the rapid growth of N deposition in East Asia, the critical loads
272 for some studied vegetation might have been exceeded before the start of the N
273 fertilization experiments, so it is not possible to observe initial changes in the ecosystem,

274 while Europe and North America have greater availability of pristine baselines (Pardo
275 et al., 2011). In addition, very limited studies and short-term observations under high
276 nitrogen dose will lead to high uncertainty of critical loads.

277 4.2 Uncertainty analysis

278 Although uncertainty did exist for the empirical N critical load range of each
279 vegetation type due to the high N addition doses, short duration of the studies, high
280 background deposition, and so on, it was difficult to quantitatively evaluate. The
281 response of ecosystem to N deposition has time lags, thus the uncertainty of short-term
282 and low nitrogen inputs studies will increase accordingly (Bobbink et al., 2015; Pardo
283 et al., 2011). Moreover, data deficiencies also increase uncertainty, e.g., fewer response
284 near the critical load of ecosystem was observed due to finite and rough N input gradient
285 (Pardo et al., 2011). In general, uncertainties are lower in places where observations at
286 the pristine end of the deposition gradient and the N addition levels are low relative
287 both to the critical load and the ambient deposition. In addition, uncertainties are lower
288 where the deposition has not increased rapidly or recently. Therefore, due to limited
289 field N fertilization experiments in East Asia, the uncertainties of empirical critical load
290 and critical load exceedance in this study may be higher than those studies in European
291 and North American, with much better databases (Pardo et al., 2011; Tipping et al.,
292 2013) Further long-term and large number of studies are necessary to reduce the
293 uncertainties.

294 By admitting uncertainties due to limited studies in East Asia, the empirical critical

295 loads provided the directions to update the calculated critical loads, e.g. by SSMB.
296 Besides Alpine steppe and Temperate grass-forb Community, the empirical critical
297 loads of forests and other grassland vegetation were usually higher than the N critical
298 loads calculated by SSMB (Table 1). The impact of N deposition on ecosystems had
299 occurred actually before it was discovered (not reaching a stable state), and the
300 empirical critical loads obtained by the direct approach was often too large. Especially
301 for subtropical forests usually with large deviations, NO_3^- leaching has obvious
302 occurred before vegetation changes. Among the responses of subtropical forests, the N
303 input required for N_2O emission was lower than the minimum N input required for
304 leaching (Huang et al., 2015; Li et al., 2015a), demonstrating the importance of
305 denitrification and N_2O emission should be considered for subtropical forests (Zhu et
306 al., 2013). Not only more reasonable parameters for denitrification should be studied
307 for the typical forests, but also new criterion (i.e., N_2O emission) instead of nitrate
308 leaching for SSMB calculation (UBA, 2004) might be sought. Since very large amount
309 of nitrate can be denitrified and removed from the ecosystem, the critical nitrate
310 leaching based on physiological response or biodiversity change of dominant species
311 always leads to higher critical loads, which may be unacceptable due to high
312 greenhouse gas emission.

313 4.3 Effects of NO_x emission reduction in China on natural ecosystems in East Asia

314 From 2010 to 2015, the deposition of nitrate (NO_3^- ; mainly from NO_x emission) in
315 China, North Korea, South Korea, and Japan decreased by 17%, 20%, 11%, and 10%,

316 respectively, according to the modeling results. However, there was little change in
317 deposition of ammonium (NH_4^+ , mainly from NH_3 emission) in East Asia (Du et al.,
318 2014; EANET, 2017). Emission abatement of NH_3 in China has not been carried out
319 and a high level of NH_3 emission remains (Zheng et al., 2018). Therefore, the reduction
320 of N deposition in East Asia was mainly attributed to NO_x emission reduction. Since
321 the emissions inventory had not changed in 2010-2015 except for China, the reduction
322 in N deposition modeled was only attributed to China's emission abatement. During
323 this period, China's NO_x emission reductions mainly came from the flue gas
324 denitrification in power plants (using selective catalytic reduction, SCR) and the
325 shutdown of small industrial boilers (Zheng et al., 2018). The reduction in emission
326 from the tall stacks was more effective for reducing long-range transported pollutants.

327 Although NH_4^+ is an important component of N deposition, NH_3 emission has not
328 been controlled globally (Hoesly et al., 2018; Kang et al., 2016). NH_4^+ and NO_3^- have
329 different biological and chemical impacts on ecosystems (Kahmen et al., 2008). For
330 example, plant and soil generally has a higher uptake and immobilization rate for NH_4^+
331 than NO_3^- (Brumme et al., 1992; Liu et al., 2017a; Ma et al., 2014; Providoli et al., 2006.
332 Puri and Ashman, 1999; Rice and Tiedje, 1989), and NH_4^+ has stronger effects of soil
333 acidification and N_2O emission than NO_3^- (Huang et al., 2015; Li et al., 2015a).
334 However, the different effects of NH_4^+ and NO_3^- have not been considered in mapping
335 empirical N critical load of nitrogen in Europe (Aherne and Posch, 2013), while the
336 threshold of atmospheric NH_3 average concentration was assigned as critical level

337 (CLE_{NH₃}) (Cape et al., 2009). In this study, the different effects of NH₄⁺ and NO₃⁻ was
338 not considered either.

339 Although critical loads may vary greatly for different ecosystems, the main reason
340 for large area of critical load exceedance is the high N deposition in the region. In
341 central and northeastern China, where temperate deciduous broad-leaved forest is
342 dominant, the empirical critical loads of nitrogen were exceeded by more than 10
343 kgN·ha⁻¹·a⁻¹ due to very high N deposition in 2010. Although N deposition was
344 relatively high in southern China, the empirical critical loads of subtropical broad-
345 leaved evergreen forest and tropical monsoon forests and rain forests were high, so
346 there was less critical load exceedance. In addition, higher critical load exceedance
347 (10~15 kgN·ha⁻¹·a⁻¹) occurred in central Japan, under the higher N deposition (10~30
348 kgN·ha⁻¹·a⁻¹). There was no critical load exceedance where the lower N deposition
349 (5~10 kgN·ha⁻¹·a⁻¹) occurred in Japan. Moreover, the higher critical load exceedance
350 (10~15 kgN·ha⁻¹·a⁻¹) occurred in some parts of north and central Korean peninsula,
351 where the N deposition is higher (20~30 kgN·ha⁻¹·a⁻¹). In 2015, with the decrease in N
352 deposition, the total area of critical load exceedance decreased by 5.33%, and to 142
353 Mha in East Asia. After the decrease in N deposition (mainly in nitrate deposition), the
354 area of critical load exceedance in the United States decreased from the peak of 178
355 Mha in 1975 to 133 Mha in 2006 (Clark et al., 2018), while it even reached 335 Mha
356 in Europe in 2010 (Slootweg et al., 2015). Studies demonstrated that the area at risk of
357 adverse effects of N deposition decreased from 67% to 61%, when NO_x and NH₃

358 emissions declined by 63% and 19% in Europe in 2030 (Hettelingh and Posch, 2019).
359 However, considering the much higher values and uncertainties of critical loads in East
360 Asia than in Europe and United States, it is too early to state that East Asia has now
361 low risk of N saturation.

362 **5. Conclusions and suggestions**

363 Controlling N deposition is critical to preventing its negative effects on natural
364 and semi-natural ecosystems. This paper provides a preliminary assessment of the risk
365 caused by high N deposition in East Asia, based on empirical N critical loads. Critical
366 load exceedances were mainly distributed in central, northeastern and some parts of
367 southern China, as well as southern and some parts of northern Korean peninsula.
368 Critical load exceedances occurred in most parts of Japan, except in small parts of
369 northern and southern Japan. The total area of critical load exceedance in East Asia was
370 142 Mha in 2015. It should be noted that the area of critical load exceedance in East
371 Asia has decreased by at least 5.33% since 2010, which showing the significant benefit
372 of NO_x emission abatement (by 17% during 2010-2017) in China.

373 It should be noted that previous studies and policy-making in East Asia paid great
374 attention to NO_x emission reduction. NH₃ emission control is also important for both
375 the improvement of air quality (to reduce PM_{2.5}) and reduction of N deposition (Liu et
376 al., 2019), and is under consideration by the Chinese government. Although the
377 empirical N critical loads derived from the published literature of N fertilization
378 experiments may give a very important scientific basis for evaluating the current status

379 of N deposition in East Asia, more long-term and well-designed field experiments
380 should be implemented in the future to further assess the impacts of different forms of
381 N deposition (not only NO₃⁻, but also NH₄⁺) on natural ecosystems, and to update the
382 empirical N critical load map.

383

384 **Acknowledgement**

385 The authors are grateful for the financial support of the National Natural Science
386 Foundation of China (41877329 and 21607091) and the Tsinghua University Initiative
387 Scientific Research Program (2015Z22029).

388

389 **References**

- 390 Aber, J., Magill, A., McNulty, S., Boone, R., Nadelhoffer, K., Downs, M., Hallett, R.,
391 1995. Forest biogeochemistry and primary production altered by nitrogen saturation.
392 *Water Air Soil Pollut.* 85, 1665-1670.
- 393 Aherne, J., Posch, M., 2013. Impacts of nitrogen and sulphur deposition on forest
394 ecosystem services in Canada. *Curr. Opin. Environ. Sustain.* 2013, 5, 108-115.
- 395 Bai, Y., Wu, J., Clark, C., Naeem, S., Pan, Q., Huang, J., Zhang, L., Han, X., 2009.
396 Tradeoffs and thresholds in the effects of nitrogen addition on biodiversity and
397 ecosystem functioning: evidence from inner Mongolia Grasslands. *Glob. Change Biol.*
398 16, 358-372.
- 399 Ban, S., Matsuda, K., Sato, K., Ohizumi, T., 2016. Long-term assessment of nitrogen
400 deposition at remote EANET sites in Japan. *Atmos. Environ.* 146, 70-78.
- 401 Bobbink, R., Roelofs, J., 1995. Nitrogen critical loads for natural and semi-natural
402 ecosystems: The empirical approach. *Water Air Soil Pollut.* 85 (4), 2413-2418.
- 403 Bobbink, R., Hicks, K., Galloway, J., Spranger, T., Alkemade, R., Ashmore, M.,
404 Bustamante, M., Cinderby, S., Davidson, E., Dentener, F., Emmett, B., Erisman, W.,
405 Fenn, M., Gilliam, F., Nordin, A., Pardo, L., de Vries, W., 2010. Global assessment of
406 nitrogen deposition effects on terrestrial plant diversity: a synthesis. *Ecol. Appl.* 20, 30-
407 59.
- 408 Bobbink, R., Braun, S., Nordin, A., Power, S., Schütz, K., Strengbom, J., Weijters, M.,
409 Tomassen, H., 2011. Review and revision of empirical critical loads and dose response

410 relationships. Proceedings of an Expert Workshop, Noordwijkerhout, 23-25.
411 Bobbink, R., Tomassen, H., Weijters, M., van den Berg, L., Strengbom, J., Braun, S.,
412 Annika, N., Schuetz, K., Hettelingh, J., 2015. Effects and Empirical Critical Loads of
413 Nitrogen for Europe. In: de Vries W., Hettelingh P., Posch M. (eds) Critical Loads and
414 Dynamic Risk Assessments. Environmental Pollution, vol 25. Springer, Dordrecht.
415 Bowman, W., Cleveland, C., Halada, L., Hresko, J., Baron, J., 2008. Negative impact
416 of nitrogen deposition on soil buffering capacity. Nat. Geosci. 1, 767-770.
417 Brumme, R., Leimcke, U., Matzner, E., 1992. Interception and uptake of NH_4^+ and
418 NO_3^- from wet deposition by aboveground parts of young beech (*Fagus sylvatica* L.)
419 trees. Plant Soil 142, 273-279.
420 Cape, J., van der Eerden, L., Sheppard, L., Leith, I., Sutton, M., 2009. Evidence for
421 changing the critical level for ammonia. Environ. Pollut. 157, 1033-7.
422 Chen, X., Mulder, J., 2007. Atmospheric deposition of nitrogen at five subtropical
423 forested sites in South China. Sci. Total Environ. 378, 317-330.
424 Chen, X., Li, Y., Mo, J., Otieno, D., Tenhunen, J., Yan, J., Zhang, D., 2012. Effects of
425 nitrogen deposition on soil organic carbon fractions in the subtropical forest ecosystems
426 of S China. J. Plant Nutr. Soil Sci. 175, 947-953.
427 Chen, H., Dong, S., Liu, L., Ma, C., Zhang, T., Zhu, X., Mo, J., 2013a. Effects of
428 experimental nitrogen and phosphorus addition on litter decomposition in an old-
429 growth tropical forest. PLoS One 8, 84101.
430 Chen, W., Zheng, X., Chen, Q., Wolf, B., Butterbach-Bahl, K., Brueggemann, N., Lin,
431 S., 2013b. Effects of increasing precipitation and nitrogen deposition on CH_4 and N_2O
432 fluxes and ecosystem respiration in a degraded steppe in Inner Mongolia, China.
433 Geoderma 192, 335-340.
434 Cheng, J., Jia, H., Peng, X., 1996. Study on vegetation community structure and its
435 succession on fertilization grassland. Research of Soil and Water Conservation 3, 124-
436 128 (in Chinese).
437 China State Council: Action Plan on Prevention and Control of Air Pollution, China
438 State Council, Beijing, China, 2013. [http://www.gov.cn/zwggk/2013-](http://www.gov.cn/zwggk/2013-09/12/content_2486773.htm)
439 [09/12/content_2486773.htm](http://www.gov.cn/zwggk/2013-09/12/content_2486773.htm) (last access: 30 September 2018).
440 CLRTAP, 2017. Manual on methodologies and criteria for modelling and mapping
441 critical loads and levels and air pollution effects, risks and trends, available at:
442 https://icpmapping.org/Latest_update_Mapping_Manual, last access: 15 August 2017.
443 Clark, C., Tilman, D., 2008. Loss of plant species after chronic low-level nitrogen
444 deposition to prairie grasslands. Nature 451, 712-715.
445 Clark, C., Phelan, J., Doraiswamy, P., Buckley, J., Cajka, J., Dennis, R., Lynch, J., Nolte,
446 C., Spero, T., 2018. Atmospheric deposition and exceedances of critical loads from
447 1800-2025 for the conterminous United States. Ecol. Appl. 28, 978-1002.
448 de Vries, W., Wamelink, G., van Dobben, H., Kros, J., Reinds, J., Mol-Dukstra, J.,
449 Smart, S., Evans, C., Rowe, E., Belyazid, S., Sverdrup, H., van Hinsberg, A., Posch,
450 M., Hettelingh, J., Spranger, T., Bobbink, R., 2010. Use of dynamic soil-vegetation
451 models to assess impacts of nitrogen deposition on plant species composition: an

452 overview. *Ecol. Appl.* 20, 60-79.

453 de Vries, W., 2015. Critical Loads and Dynamic Risk Assessments: Nitrogen, Acidity
454 and Metals in Terrestrial and Aquatic Ecosystems.

455 Du, E., Zhou, Z., Li, P., Hu, X., Ma, Y., Wang, W., Fang, J., 2013. NEECF: a project of
456 nutrient enrichment experiments in China's forests. *J. Plant Ecol.* 6, 428-435.

457 Du, E., Fang, J., 2014. Weak growth response to nitrogen deposition in an old-growth
458 boreal forest. *Ecosphere* 5, 1-9.

459 Du, E., Jiang, Y., Fang, J., de Vries, W., 2014. Inorganic nitrogen deposition in China's
460 forests: Status and characteristics. *Atmos. Environ.* 98, 474-482.

461 Du, E., 2016. Rise and fall of nitrogen deposition in the United States. *Proc. Natl. Acad.*
462 *Sci. U. S. A.* 113, E3594-5.

463 Duan, L., Xie, S., Zhou, Z., Ye, X., Hao, J., 2001. Calculation and mapping of critical
464 loads for S, N and acidity in China. *Water Air Soil Pollut.* 130, 1199-1204.

465 Duan, L., Xing, J., Zhao, Y., Hao, J., 2014. Empirical Critical Loads of Nitrogen in
466 China. In: Sutton M, Mason K, Sheppard L, Sverdrup H, Haeuber R, Hicks WK (eds).
467 Nitrogen Deposition, Critical Loads and Biodiversity. Springer Netherlands.

468 Duan, L., Yu, Q., Zhang, Q., Wang, Z., Pan, Y., Larssen, T., Mulder, J., 2016. Acid
469 deposition in Asia: Emissions, deposition, and ecosystem effects. *Atmos. Environ.* 146,
470 55-69.

471 EANET, 2017. Data Report 2017. Acid Deposition Monitoring Network in East
472 Asia. <https://monitoring.eanet.asia/document/public/index>

473 Endo, T., Yagoh, H., Sato, K., Matsuda, K., Hayashi, K., Noguchi, I., Sawada, K., 2011.
474 Regional characteristics of dry deposition of sulfur and nitrogen compounds at EANET
475 sites in Japan from 2003 to 2008. *Atmos. Environ.* 45, 1259-1267.

476 FAO (Food and Agriculture Organization), 2010.
477 [http://www.fao.org/geonetwork/srv/en/main.home?uuid=c2639320-88fd-11da-a88f-](http://www.fao.org/geonetwork/srv/en/main.home?uuid=c2639320-88fd-11da-a88f-000d939bc5d8)
478 [000d939bc5d8](http://www.fao.org/geonetwork/srv/en/main.home?uuid=c2639320-88fd-11da-a88f-000d939bc5d8)

479 Fan, H., Liu, W., Li, Y., Liao, Y., Yuan, Y., Xu, L., 2007a. Tree growth and soil nutrients
480 in response to nitrogen deposition in a subtropical Chinese fir plantation. *Acta*
481 *Ecologica Sinica* 27, 4630-4642 (in Chinese).

482 Fan, H., Liu, W., Qiu, X., Xu, L., Wang, Q., Chen, Q., 2007b. Responses of litterfall
483 production in Chinese fir plantation to increased nitrogen deposition. *Journal of*
484 *Ecology* 26, 1335-1338 (in Chinese).

485 Fan, H., Liu, W., Xu, L., Li, Y., Liao, Y., Wang, Q., Zhang, Z., 2008. Carbon and
486 nitrogen dynamics of decomposing foliar litter in a Chinese fir (*Cunninghamia*
487 *lanceolata*) plantation exposed to simulated nitrogen deposition. *Acta Ecologica Sinica*
488 28, 2546-2553 (in Chinese).

489 Fang, Y., Mo, J., Zhou, G., Xue, J., 2005. Response of diameter at breast height
490 increment to N additions in forests of Dinghushan Biosphere Reserve. *Journal of*
491 *Tropical and Subtropical Botany* 13, 198-204 (in Chinese).

492 Fang, Y., Yoh, M., Mo, J., Gundersen, P., Zhou, G., 2009. Response of nitrogen leaching
493 to nitrogen deposition in disturbed and mature forests of Southern China. *Pedosphere*

494 19, 111-120.

495 Fang, H., Cheng, S., Yu, G., Cooch, J., Wang, Y., Xu, M., Li, L., Dang, X., Li, Y., 2014.

496 Low-level nitrogen deposition significantly inhibits methane uptake from an alpine

497 meadow soil on the Qinghai–Tibetan Plateau. *Geoderma* 213, 444-452.

498 Fagerli, H., Aas, W., 2008. Trends of nitrogen in air and precipitation: Model results

499 and observations at EMEP sites in Europe, 1980-2003. *Environ. Pollut.* 154 (3), 448-

500 461.

501 Gao, Y., He, N., Zhang, X., 2014. Effects of reactive nitrogen deposition on terrestrial

502 and aquatic ecosystems. *Ecol. Eng.* 70, 312-318.

503 Gao, W., Kou, L., Zhang, J., Müller, C., Yang, H., Li, S., 2016. Ammonium fertilization

504 causes a decoupling of ammonium cycling in a boreal forest. *Soil Biol. Biochem.* 101,

505 114-123.

506 Galloway, J., 2005. The global nitrogen cycle: Past, present and future. *Science in*

507 *China Series C-Life Sciences* 48, 669-677.

508 Geiser, L., Nelson, P., Jovan, S., Root, H., Clark, C., 2019. Assessing Ecological Risks

509 from Atmospheric Deposition of Nitrogen and Sulfur to US Forests Using Epiphytic

510 Macrolichens. *Diversity-Basel*, 11 (6), 87.

511 Gilliam, F., 2006. Response of the herbaceous layer of forest ecosystems to excess

512 nitrogen deposition. *J. Ecol.* 94, 1176–1191.

513 Guenther, A., Karl, T., Harley, P., Wiedinmyer, C., Palmer, P., Geron, C., 2006.

514 Estimates of global terrestrial isoprene emissions using MEGAN (Model of Emissions

515 of Gases and Aerosols from Nature). *Atmos. Chem. Phys.* 6, 3181-3210.

516 Hao, J., Duan, L., Zhou, X., Fu, L., 2001. Application of a LRT Model to acid rain

517 control in China. *Environ. Sci. Technol.* 35, 3407-3415.

518 He, K., Qi, Y., Huang, Y., Chen, H., Sheng, Z., Xu, X., Duan, L., 2016. Response of

519 aboveground biomass and diversity to nitrogen addition - a five-year experiment in

520 semi-arid grassland of Inner Mongolia, China. *Sci Rep* 6, 31919.

521 Hettelingh, J., Posch, M., de Smet, P., Downing, R., 1995. The use of critical loads in

522 emission reduction agreement in Europe. *Water Air Soil Pollut.* 85, 2381-2388.

523 Hettelingh, J., Posch, M., Slootweg, J., 2009. Critical Load, Dynamic Modelling and

524 Impact Assessment in Europe: CCE Status Report 2008. Coordination Centre for

525 Effects, Netherlands Environmental Assessment Agency.

526 Hettelingh, J., Posch, M., 2019 Critical load exceedances under equitable nitrogen

527 emission reductions in the EU28. *Atmos. Environ.* 211, 113-119.

528 Hogberg, P., Fan, H., Quist, M., Binkley, D., Tamm, C., 2006. Tree growth and soil

529 acidification in response to 30 years of experimental nitrogen loading on boreal forest.

530 *Glob. Change Biol.* 12, 489-499.

531 Hoesly, R., Smith, S., Feng, L., Klimont, Z., Janssens-Maenhout, G., Pitkanen, T.,

532 Seibert, J., J.; Linh, V., Andres, R., Bolt, R., Bond, T., Dawidowski, L., Kholod, N.,

533 Kurokawa, J., Li, M., Liu, L., Lu, Z., Moura, M., O'Rourke, P., Zhang, Q., 2018.

534 Historical (1750-2014) anthropogenic emissions of reactive gases and aerosols from
535 the Community Emissions Data System (CEDS). *Geosci. Model Dev.* 11 (1), 369-
536 408.

537 Hu, Y., Zeng, D., Liu, Y., Zhang, Y., Chen, Z., Wang, Z., 2010. Responses of soil
538 chemical and biological properties to nitrogen addition in a Dahurian larch plantation
539 in Northeast China. *Plant Soil* 333, 81-92.

540 Huang, Y., Kang, R., Mulder, J., Zhang, T., Duan, L., 2015. Nitrogen saturation, soil
541 acidification, and ecological effects in a subtropical pine forest on acid soil in southwest
542 China. *J. Geophys. Res.-Biogeosci.* 120, 2457-2472.

543 ICP M & M (2010). Manual on Methodologies and Criteria for Modelling and Mapping
544 Critical Loads & levels and Air Pollution Effects, Risks and Trends, update of UBA
545 (2004) in prep., www.icpmapping.org

546 Jia, S., Wang, Z., Li, X., Sun, Y., Zhang, X., Liang, A., 2010. N fertilization effects on
547 soil respiration, microbial biomass and root respiration in *Larix gmelinii* and *Fraxinus*
548 *mandshurica* plantations in China. *Plant Soil* 333, 325-336.

549 Jiang, C., Yu, G., Fang, H., Cao, G., Li, Y., 2010. Short-term effect of increasing
550 nitrogen deposition on CO, CH and NO fluxes in an alpine meadow on the Qinghai-
551 Tibetan Plateau, China. *Atmos. Environ.* 44, 2920-2926.

552 Jiang, L., Tian, D., Ma, S., Zhou, X., Xu, L., Zhu, J., Jing, X., Zheng, C., Shen, H.,
553 Zhou, Z., 2017. The response of tree growth to nitrogen and phosphorus additions in a
554 tropical montane rainforest. *Sci. Total Environ.* 618, 1064-1070.

555 Kahmen, A., Wanek, W., Buchmann, N., 2008. Foliar $\delta^{15}\text{N}$ values characterize soil N
556 cycling and reflect nitrate or ammonium preference of plants along a temperate
557 grassland gradient. *Oecologia* 156, 861-870.

558 Kang, Y., Liu, M., Song, Y., Huang, X., Yao, H., Cai, X., Zhang, H., Kang, L., Liu, X.,
559 Yan, X., He, H., Zhang, Q., Shao, M., Zhu, T., 2016. High-resolution ammonia
560 emissions inventories in China from 1980 to 2012. *Atmos. Chem. Phys.* 16 (4), 2043-
561 2058.

562 Kreuzer, K., Butterbach-Bahl, K., Rennenberg, H., Papen, H., 2009. The complete
563 nitrogen cycle of an N-saturated spruce forest ecosystem. *Plant Biol.* 11, 643-649.

564 Kim, M., Imori, M., Watanabe, M., Hatano, R., Yi, M., Koike, T., 2012. Simulated
565 nitrogen inputs influence methane and nitrous oxide fluxes from a young larch
566 plantation in northern Japan. *Atmos. Environ.* 46, 36-44.

567 Kong, Y., Watanabe, M., Nagano, H., Watanabe, K., Yashima, M., Inubushi, K., 2013.
568 Effects of land-use type and nitrogen addition on nitrous oxide and carbon dioxide
569 production potentials in Japanese Andosols. *Soil Sci. Plant Nutr.* 59, 790-799.

570 Kurokawa, J., Ohara, T., Morikawa, T., Hanayama, S., Janssens-Maenhout, G., Fukui,
571 T., Kawashima, K., Akimoto, H., 2013. Emissions of air pollutants and greenhouse
572 gases over Asian regions during 2000–2008: Regional Emission inventory in Asia
573 (REAS) version 2. *Atmos. Chem. Phys.* 13, 11019-11058.

574 Larssen, T., Lydersen, E., Tang, D., He, Y., Gao, J., Liu, H., Duan, L., Seip, H., Vogt,
575 R., Mulder, J., Shao, M., Wang, Y., Shang, H., Zhang, X., Solberg, S., Aas, W., Okland,

576 T., Eilertsen, O., Angell, V., Li, Q., Zhao, D., Xiang, R., Xiao, J., Luo, J., 2006. Acid
577 rain in China. *Environ. Sci. Technol.* 40, 418-425.

578 Lan, Z., Bai, Y., 2012. Testing mechanisms of N-enrichment-induced species loss in a
579 semiarid Inner Mongolia grassland: critical thresholds and implications for long-term
580 ecosystem responses. *Philosophical Transactions of the Royal Society B: Biological
581 Sciences* 367, 3125-3134.

582 Lee, J., Nakamura, M., Hiura, T., 2017. Does large-scale N fertilization have time-
583 delayed effects on insects community structure by changing oak quantity and quality?
584 *Arthropod-Plant Interact.* 11, 515-523.

585 Li, X., Zheng, X., Han, S., Zheng, J., Li, T., 2010. Effects of nitrogen additions on
586 nitrogen resorption and use efficiencies and foliar litterfall of six tree species in a mixed
587 birch and poplar forest, northeastern China. *Can. J. For. Res.* 40, 2256-2261.

588 Li, K., Gong, Y., Song, W., He, G., Hu, Y., 2012a. Responses of CH₄, CO₂ and N₂O
589 fluxes to increasing nitrogen deposition in alpine grassland of the Tianshan Mountains.
590 *Chemosphere* 88, 140-143.

591 Li, K., Gong, Y., Song, W., Lv, J., Chang, Y., 2012b. No significant nitrous oxide
592 emissions during spring thaw under grazing and nitrogen addition in an alpine grassland.
593 *Glob. Change Biol.* 18, 2546–2554.

594 Li, X., Cheng, S., Fang, H., Yu, G., Dang, X., Xu, M., Wang, L., Si, G., Geng, J., He,
595 S., 2015a. The contrasting effects of deposited NH₄⁺ and NO₃⁻ on soil CO₂, CH₄ and
596 N₂O fluxes in a subtropical plantation, southern China. *Ecol. Eng.* 85, 317-327.

597 Li, K., Liu, X., Song, L., Gong, Y., Lu, C., 2015b. Response of alpine grassland to
598 elevated nitrogen deposition and water supply in China. *Oecologia* 177, 65-72.

599 Li, M., Zhang, Q., Kurokawa, J., Woo, J., He, K., Lu, Z., Ohaea, T., Song, Y., Streets,
600 D., Carmichael, G., Cheng, Y., Hong, C., Huo, H., Jiang, X., Kand, S., Liu, F., Su, H.,
601 Zheng, B., 2017. MIX: a mosaic Asian anthropogenic emission inventory under the
602 international collaboration framework of the MICS-Asia and HTAP. *Atmos. Chem.
603 Phys.* 17, 935-963.

604 Lin, Y., Duan, L., Yang, Y., Zhao, D., Zhang, D., Hao, J., 2007. Contribution of
605 simulated nitrogen deposition to forest soil acidification in area with high sulfur
606 deposition. *Environmental Science*, 28, 640-646 (in Chinese).

607 Liu, W., Fan, H., Zhang, Z., Yang, Y., Wang, Q., Xu, L., 2008. Foliar nutrient contents
608 of Chinese fir in response to simulated nitrogen deposition. *Chinese Journal of Applied
609 and Environmental Biology* 14, 319-323 (in Chinese).

610 Liu, X., Duan, L., Mo, J., Du, E., Shen J., Lu X.i, Zhang Y., Zhou X., He C., Zhang F.,
611 2011. Nitrogen deposition and its ecological impact in China: an overview. *Environ.
612 Pollut.* 2011, 159: 2251-2264.

613 Liu, J., Huang, W., Zhou, G., Zhang, D., Liu, S., Li, Y., 2013a. Nitrogen to phosphorus
614 ratios of tree species in response to elevated carbon dioxide and nitrogen addition in
615 subtropical forests. *Glob. Change Biol.* 19, 208-216.

616 Liu, Y., Xu, R., Xu, X., Wei, D., Wang, Y., 2013b. Plant and soil responses of an alpine
617 steppe on the Tibetan Plateau to multi-level nitrogen addition. *Plant Soil* 373, 515-529.

618 Liu, W., Yu, L., Zhang, T., Kang, R., Zhu, J., Mulder, J., Duan, L., 2017a. In situ ¹⁵N
619 labeling experiment reveals different long-term responses to ammonium and nitrate
620 inputs in N-saturated subtropical forest. *J. Geophys. Res.-Biogeosci.* 122, 2251–2264.
621 Liu, X., Zhang, Q., Li, S., Zhang, L., Ren, J., 2017b. Simulated NH₄⁺ -N Deposition
622 Inhibits CH₄ Uptake and Promotes N₂O Emission in the Meadow Steppe of Inner
623 Mongolia, China. *Pedosphere* 27, 306-317.
624 Liu, M., Huang, X., Song, Y., Tang, J., Cao, J., Zhang, X., Zhang, Q., Wang, S., Xu, T.,
625 Kang, L., Cai, X., Zhang, H., Yang, F., Wang, H., Yu, J., Lau, A., He, L., Huang, X.,
626 Duan, L., Ding, A., Xue, L., Gao, J., Liu, B., Zhu, T., 2019. Ammonia emission control
627 in China would mitigate haze pollution and nitrogen deposition, but worsen acid rain.
628 *Proc. Natl. Acad. Sci. U. S. A.* doi:10.1073/pnas.1814880116.
629 Lu, X., Mo, J., Peng, S., Fang, Y., Li, D., Lin, Q., 2006. Effects of simulated N
630 deposition on free amino acids and soluble protein of three dominant understory species
631 in a monsoon evergreen broad-leaved forest of subtropical China. *Acta Ecologica*
632 *Sittica* 26, 743-753 (in Chinese).
633 Lu, X., Mo, J., Li, D., Zang, W., Fang, Y., 2007. Effects of simulated N deposition on
634 the photosynthetic and physiologic characteristics of dominant understory plants in
635 Dinghushan Mountain of subtropical China. *Journal of Beijing Forestry University* 29,
636 1-9 (in Chinese).
637 Lu, X., Mo, J., Gilliam, F., Zhou, G., Fang, Y., 2010. Effects of experimental nitrogen
638 additions on plant diversity in an old-growth tropical forest. *Glob. Change Biol.* 16,
639 2688-2700.
640 Lu, X., Gilliam, F., Yu, G., Li, L., Mao, Q., Chen, H., Mo, J., 2013. Long-term nitrogen
641 addition decreases carbon leaching in a nitrogen-rich forest ecosystem. *Biogeosciences*
642 10, 3931-3941.
643 Lu, X., Mao, Q., Gilliam, F., Luo, Y., Mo, J., 2014. Nitrogen deposition contributes to
644 soil acidification in tropical ecosystems. *Glob. Change Biol.* 20, 3790-3801.
645 Lynch, J., Pardo, L., Huber, C., 2013. Detailed documentation of the CLAD U.S.
646 Critical Loads of Sulfur and Nitrogen Access Database, version 2.0. Created for the
647 Critical Loads of Atmospheric Deposition (CLAD) Science Subcommittee of the
648 National Atmospheric Deposition Program (NADP). [http://nadp.](http://nadp.sws.uiuc.edu/claddb/dl/CLAD_DBV2_Final.pdf)
649 [sws.uiuc.edu/claddb/dl/CLAD_DBV2_Final.pdf](http://nadp.sws.uiuc.edu/claddb/dl/CLAD_DBV2_Final.pdf)
650 Ma, K., Sheng, W., Yu, G., Fang, H., Jiang, C., Yan, J., Zhou, M., 2014. Sinks for
651 Inorganic Nitrogen Deposition in Forest Ecosystems with Low and High Nitrogen
652 Deposition in China. *PLoS One* 9, e89332.
653 Mao, Q., Lu, X., Zhou, K., Chen, H., Zhu, X., Mori, T., Mo, J., 2017. Effects of long-
654 term nitrogen and phosphorus additions on soil acidification in an N-rich tropical forest.
655 *Geoderma* 285, 57-63.
656 McNulty, S., Cohen, E., Moore, J., 2013. Climate Change Impacts on Forest Soil
657 Critical Acid Loads and Exceedances at a National Scale. In: Potter, Kevin M.;
658 Conkling, Barbara L., eds. 2013. *Forest Health Monitoring: national status, trends, and*
659 *analysis 2010. Gen. Tech. Rep. SRS-GTR-176.*

660 MEP (Ministry of Environmental Protection of China), 2011. Ecological Environment
661 Bulletin of China.
662 [http://www.zhb.gov.cn/hjzl/zghjzkgb/lnzghjzkgb/201805/P020180531534645032372.](http://www.zhb.gov.cn/hjzl/zghjzkgb/lnzghjzkgb/201805/P020180531534645032372.pdf)
663 pdf
664 Ministry of Environment of Japan, 2014. <http://www.env.go.jp/air/osen/law/index.html>.
665 Mijling, B., van der A, J., Zhang, Q., 2013. Regional nitrogen oxides emission trends
666 in East Asia observed from space. *Atmos. Chem. Phys.* 13, 12003-12012.
667 Morino, Y., Ohara, T., Kurokawa, J., Kuribayashi, M., Uno, I., Hara, H., 2011.
668 Temporal variations of nitrogen wet deposition across Japan from 1989 to 2008. *J.*
669 *Geophys. Res.* 2011, 116, 1-17.
670 NEG-ECP, 2001. Critical Load of Sulphur and Nitrogen Assessment and Mapping
671 Protocol for Upland Forests. New England Governors and eastern Canadian Premiers
672 Environment Task Group, Acid Rain Action Plan, Halifax, Canada, 2001.
673 Nilsson, J., Grennfelt, P., 1988. Critical loads for sulphur and nitrogen. Report from a
674 Workshop held at Skokloster Sweden March 19–24 1988. Miljø rapport 1988: 15.
675 Copenhagen Denmark Nordic Council of Ministers.
676 Pan, Q., Bai, Y., Han, X., Zhang, L., 2004. Carbohydrate reserves in the rhizome of
677 *Leymus chinensis* in response to nitrogen additions. *Acta Phytocologica Sinica* 28, 53-
678 58 (in Chinese).
679 Pan, Q., Bai, Y., Han, X., Yang, J., 2005. Effects of nitrogen additions on a *leymus*
680 *chinensis* population in typical steppe of Inner Mongolia. *Acta Phytocologica Sinica*
681 29, 311-317 (in Chinese).
682 Park, S., Bashkin, V., 2001. Sulfur acidity loading in South Korean ecosystems. *Water*
683 *Air Soil Pollut.* 132, 19-41.
684 Pardo, L., Fenn, M., Goodale, C., Geiser, L., Driscoll, C., Allen, E., Baron, J., Bobbink,
685 R., Bowman, W., Clark, C., Emmett, B., Gilliam, F., Greaver, T., Hall, S., Lilleskov, E.,
686 Liu, L., Lynch, J., Nadelhoffer, K., Perakis, S., Robin-Abbott, M., Stoddard, J.,
687 Weathers, K., Dennis, R., 2011. Effects of nitrogen deposition and empirical nitrogen
688 critical loads for ecoregions of the United States. *Ecol. Appl.* 21, 3049-3082.
689 Peng, Y., Chen, G., Chen, G., Li, S., Peng, T., Qiu, X., Tu, L., 2017. Soil biochemical
690 responses to nitrogen addition in a secondary evergreen broad-leaved forest ecosystem.
691 *Sci. Rep.* 7, 1-11.
692 Posch, M., de Smet, M., Hettelingh, J., Downing, R., 2001. Modelling and mapping of
693 critical thresholds in Europe. Status report 2001. RIVM Report Number 259101010.
694 Coordination Center for Effects, National Institute for Public Health and the
695 Environment, Bilthoven, The Netherlands. <http://www.mnp.nl/cce/publ/i>
696 Posch, M., Duan, L., Reinds, G., Zhao, Y., 2014. Critical loads of nitrogen and sulphur
697 to avert acidification and eutrophication in Europe and China. *Landsc. Ecol.* 30, 487-
698 499.
699 Providoli, I., Bugmann, H., Siegwolf, R., Buchmann, N., Schleppei, P., 2006. Pathways
700 and dynamics of $^{15}\text{NO}_3^-$ and $^{15}\text{NH}_4^+$ applied in a mountain *Picea abies* forest and in a
701 nearby meadow in central Switzerland. *Soil Biol. Biochem.* 38, 1645–1657.

702 Puri, G., Ashman, M., 1999. Microbial immobilization of ¹⁵N-labelled ammonium and
703 nitrate in a temperate woodland soil. *Soil Biol. Biochem.* 31, 929–931.

704 Rice, C., Tiedje, J., 1989. Regulation of nitrate assimilation by ammonium in soils
705 and in isolated soil microorganisms. *Soil Biol. Biochem.* 21, 597–602.

706 Qin, P., Qi, Y., Dong, Y., Xiao, S., He, Y., 2011. Soil nitrous oxide emissions from a
707 typical semiarid temperate steppe in Inner Mongolia: effects of mineral nitrogen
708 fertilizer levels and forms. *Plant Soil* 342, 345-357.

709 Schwede, D., Simpson, D., Tan, J., Fu, J., Dentener, F., Du, E., deVries, W., 2018.
710 Spatial variation of modelled total, dry and wet nitrogen deposition to forests at global
711 scale. *Environ. Pollut.* 243, 1287-1301.

712 Silvertown, J., Poulton, P., Johnston, A., Edwards, G., Heard, M., Biss, P., 2006. The
713 Park grass experiment 1856-2006: its contribution to ecology. *J. Ecol.* 94, 801-814.

714 Slootweg, J., Posch, M., Hettelingh, J (eds.), 2015. Modelling and mapping the impacts
715 of atmospheric deposition of nitrogen and sulphur: CCE Status Report 2015,
716 Coordination Centre for Effects, www.wge-cce.org.

717 Song, L., Bao, X., Liu, X., Zhang, Y., Christie, A., Fangmeier, A., Zhang, F., 2011.
718 Nitrogen enrichment enhances the dominance of grasses over forbs in a temperate
719 steppe ecosystem. *Biogeosciences* 8, 2341-2350.

720 Song, L., Tian, P., Zhang, J., Jin, G., 2017. Effects of three years of simulated nitrogen
721 deposition on soil nitrogen dynamics and greenhouse gas emissions in a Korean pine
722 plantation of northeast China. *Sci. Total Environ.* 609, 1303-1311.

723 Tian, Q., Liu, N., Bai, W., Li, L., Chen, J., Reich, P., Yu, Q., Guo, D., Smith, M., Knapp,
724 A., Cheng, W., Lu, P., Gao, Y., Yang, A., Wang, T., Li, X., Wang, Z., Ma, Y., Han, X.,
725 Zhang, W., 2016. A novel soil manganese mechanism drives plant species loss with
726 increased nitrogen deposition in a temperate steppe. *Ecology* 97, 65-74

727 Tian, D., Jiang, L., Ma, S., Fang, W., Schmid, B., Xu, L., Fang, J., 2017a. Effects of
728 nitrogen deposition on soil microbial communities in temperate and subtropical forests
729 in China. *Sci. Total Environ.* 607-608, 1367-1375.

730 Tian, D., Li, P., Fang, W., Xu, J., Luo, Y., Yan, Z., Fang, J., 2017b. Growth responses
731 of trees and understory plants to nitrogen fertilization in a subtropical forest in China.
732 *Biogeosciences* 14, 3461-3469.

733 Tipping, E., Henrys, P., Maskell, L., Smart, S., 2013. Nitrogen deposition effects on
734 plant species diversity; threshold loads from field data. *Environ. Pollut.* 179, 218-223.

735 Theobald, M., Vivanco, M., Aas, W., Andersson, C., Ciarelli, G., Couvidat, F., Cuvelier,
736 K., Manders, A., Mircea, M., Pay, M., Tsyro, S., Adani, M., Bergstrom, R., Bessagnet,
737 B., Briganti, G., Cappelletti, A., D'Isidoro, M., Fagerli, H., Mar, K., Otero, N., Raffort,
738 V., Roustan, Y., Schaap, M., Wind, P., Colette, A., 2019. An evaluation of European
739 nitrogen and sulfur wet deposition and their trends estimated by six chemistry transport
740 models for the period 1990-2010. *Atmos. Chem. Phys.* 19 (1), 379-405.

741 UBA(Ed.), 2004. Manual on Methodologies and Criteria for Modelling and Mapping
742 Critical Loads and Levels, and Air Pollution Effects, Risks and Trends. German Federal
743 Environmental Agency, Berlin, Germany. www.icpmapping.org.

744 Vet, R., Artz, R., Carou, S., Shaw, M., Ro, C., Aas, W., Reid, N., 2014. A global
745 assessment of precipitation chemistry and deposition of sulfur, nitrogen, sea salt, base
746 cations, organic acids, acidity and pH, and phosphorus. *Atmos. Environ.* 93, 3-100.

747 Wan, H., Yang, Y., Bai, S., Xu, Y., Bai, Y., 2008. Variations in leaf functional traits of
748 six species along a nitrogen addition gradient in *leymus chinensis* steppe in inner
749 Mongolia. *Journal of Plant Ecology* 32, 611-621 (in Chinese).

750 Wang, S., Zhao, B., Cai, S., Klimont, Z., Nielsen, P., Morikawa, T., Woo, J., Kim, Y.,
751 Fu, X., Xu, J., Hao, J., He, K., 2014. Emission trends and mitigation options for air
752 pollutants in East Asia, *Atmos. Chem. Phys.* 14, 6571-6603.

753 Wang, X., Agathokleous, E., Qu, L., Fujita, S., Watanabe, M., Tamai, Y., Mao, Q.,
754 Koyama, A., Koike, T., 2018. Effects of simulated nitrogen deposition on
755 ectomycorrhizae community structure in hybrid larch and its parents grown in volcanic
756 ash soil: The role of phosphorous. *Sci. Total Environ.* 618, 905-915.

757 Wei, D., Xu, R., Liu, Y., Wang, Y., Wang, Y., 2014. Three-year study of CO₂, efflux
758 and CH₄/N₂O fluxes at an alpine steppe site on the central Tibetan Plateau and their
759 responses to simulated N deposition. *Geoderma* 232-234, 88-96.

760 Wu, J., Liu, W., Fan, H., Huang, G., Wan, S., Yuan, Y., Ji, C., 2013. Asynchronous
761 responses of soil microbial community and understory plant community to simulated
762 nitrogen deposition in a subtropical forest. *Ecol. Evol.* 3, 3895-3905.

763 Xie, D., Zhang, T., Yu, Q., Huang, Y., Mulder, J., Duan, L., 2018a. A sharp decline in
764 nitrogen input in a N-saturated subtropical forest causes an instantaneous reduction in
765 nitrogen leaching. *J. Geophys. Res.-Biogeosci.* 123 (10), 3320-3330.

766 Xie, D., Si, G., Zhang, T., Mulder, J., Duan, L., 2018b. Nitrogen deposition increases
767 N₂O emission from an N-saturated subtropical forest in southwest China. *Environ.*
768 *Pollut.* 243, 1818-1824.

769 Xu, G., Mo, J., Zhou, G., Xue, J., 2005. Litter decomposition under N deposition in
770 Dinghushan forests and its relationship with soil fauna. *Ecology and Environment* 14,
771 901-907 (in Chinese).

772 Xu, W., Luo, X., Pan, Y., Zhang, L., Tang, A., Shen, J., Liu, X., 2015. Quantifying
773 atmospheric nitrogen deposition through a nationwide monitoring network across
774 China. *Atmos. Chem. Phys.* 15, 12345-12360.

775 Xu, Z., Ren, H., Li, M., Brunner, I., Yin, J., Liu, H., Jiang, Y., 2017. Experimentally
776 increased water and nitrogen affect root production and vertical allocation of an old-
777 field grassland. *Plant Soil* 412, 369-380.

778 Yan, Y., Ganjurjav, H., Hu, G., Liang, Y., Li, Y., He, S., Dan, L., Yang, J., Gao, Q., 2018.
779 Nitrogen deposition induced significant increase of N₂O emissions in a dry alpine
780 meadow on the central Qinghai-Tibetan Plateau. *Agric. Ecosyst. Environ.* 265, 45-53.

781 Yang, K., Zhu, J., Gu, J., Yu, L., Wang, Z., 2015. Changes in soil phosphorus fractions
782 after 9 years of continuous nitrogen addition in a *Larix gmelinii* plantation. *Ann. For.*
783 *Sci.* 72, 435-442.

784 Yang, K., Zhu, J., Gu, J., Xu, S., Yu, L., Wang, Z., 2018. Effects of continuous nitrogen
785 addition on microbial properties and soil organic matter in a *Larix gmelinii* plantation

786 in China. *J. For. Res.* 29, 85-92.

787 Zhao, Y., Li, X., Han, S., Hu, Y., 2008. Soil enzyme activities under two forest types as
788 affected by different levels of nitrogen deposition. *Chinese Journal of Applied Ecology*
789 19, 2769-2773 (in Chinese).

790 Zhao, Y., Duan, L., Xing, J., Larssen, T., Nielsen, C., Hao, J., 2009a. Soil acidification
791 in China: Is controlling SO₂ emissions enough? *Environ. Sci. Technol.* 43, 8021-8026.

792 Zhao, Y., Han, S., Li, X., Hu, Y., 2009b. Effect of Simulated nitrogen deposition on soil
793 microbial biomass. *Journal of Northeast Forestry University* 37, 49-51 (in Chinese).

794 Zhao, B., Wang, S., Liu, H., Xu, J., Fu, K., Klimont, Z., Hao, J., He, K., Cofala, J.,
795 Amann, M., 2013. NO_x emissions in China: Historical trends and future perspectives.
796 *Atmos. Chem. Phys.* 13, 9869-9897.

797 Zhao, B., Wang, S., Donahue, N., Jathar, S., Huang, X., Wu, W., Hao, J., Robinson, A.,
798 2016. Quantifying the effect of organic aerosol aging and intermediate-volatility
799 emissions on regional-scale aerosol pollution in China. *Sci Rep* 6, 28815.

800 Zhao, Y., Zhang, L., Chen, Y., Liu, X., Xu, W., Pan, Y., Duan, L., 2017a. Atmospheric
801 nitrogen deposition to China: A model analysis on nitrogen budget and critical load
802 exceedance. *Atmos. Environ.* 153, 32-40.

803 Zhao, B., Wu, W., Wang, S., Xing, J., Chang, X., Liu, K., Jiang, J., Gu, Y., Jang, C., Fu,
804 J., Zhu, Y., Wang, J., Lin, Y., Hao, J., 2017b. A modeling study of the nonlinear response
805 of fine particles to air pollutant emissions in the Beijing-Tianjin-Hebei region. *Atmos.*
806 *Chem. Phys.* 17, 12031-12050.

807 Zhao, B., Zheng, H., Wang, S., Smith, K., Lu, X., Aunan, K., Gu, Y., Wang, Y., Ding,
808 D., Xing, J., Fu, X., Yang, X., Liu, K., Hao, J., 2018. Change in household fuels
809 dominates the decrease in PM_{2.5} exposure and premature mortality in China in 2005-
810 2015. *Proc. Natl. Acad. Sci. U. S. A.* 115, 12401-12406.

811 Zhang, Y., Shen, Y., Liu, W., 2004. Fertilization effects of N and P on a grass
812 community at the dry valley of Jinsha River. *Bulletin of Botanical Research* 24, 59-64
813 (in Chinese).

814 Zhang, Q., Streets, G., Carmichael, R., He, K., Huo, H., Kannari, A., Klimont, Z., Park,
815 I., Reddy, S., Fu, J., Chen, D., Duan, L., Lei, Y., Wang, L., Yao, Z., 2009. Asian
816 emissions in 2006 for the NASA INTEX-B mission. *Atmos. Chem. Phys.* 9, 5131-5153.

817 Zhang, J., Ai, Z., Liang, C., Wang, G., Xue, S., 2017. Response of soil microbial
818 communities and nitrogen thresholds of *Bothriochloa ischaemum* to short-term
819 nitrogen addition on the Loess Plateau. *Geoderma* 308, 112-119.

820 Zhu, J., Mulder, J., Bakken, L., Dorsch, P., 2013. The importance of denitrification for
821 N₂O emissions from an N-saturated forest in SW China: results from in situ N-15
822 labeling experiments. *Biogeochemistry* 116, 103-117.

823 Zhu, J., He, N., Wang, Q., Yuan, G., Wen, D., Yu, G., Jia, Y., 2015. The composition,
824 spatial patterns, and influencing factors of atmospheric wet nitrogen deposition in
825 Chinese terrestrial ecosystems. *Sci. Total Environ.* 511, 777-785.

826 Zheng, B., Tong, D., Li, M., Liu, F., Hong, C., Geng, G., Li, H., Li, X., Peng, L., Qi, J.,
827 Yan, L., Zhang, Y., Zhao, H., Zheng, Y., He, K., Zhang, Q., 2018. Trends in China's

828 anthropogenic emissions since 2010 as the consequence of clean air actions. Atmos.
829 Chem. Phys. 18, 14095-14111.

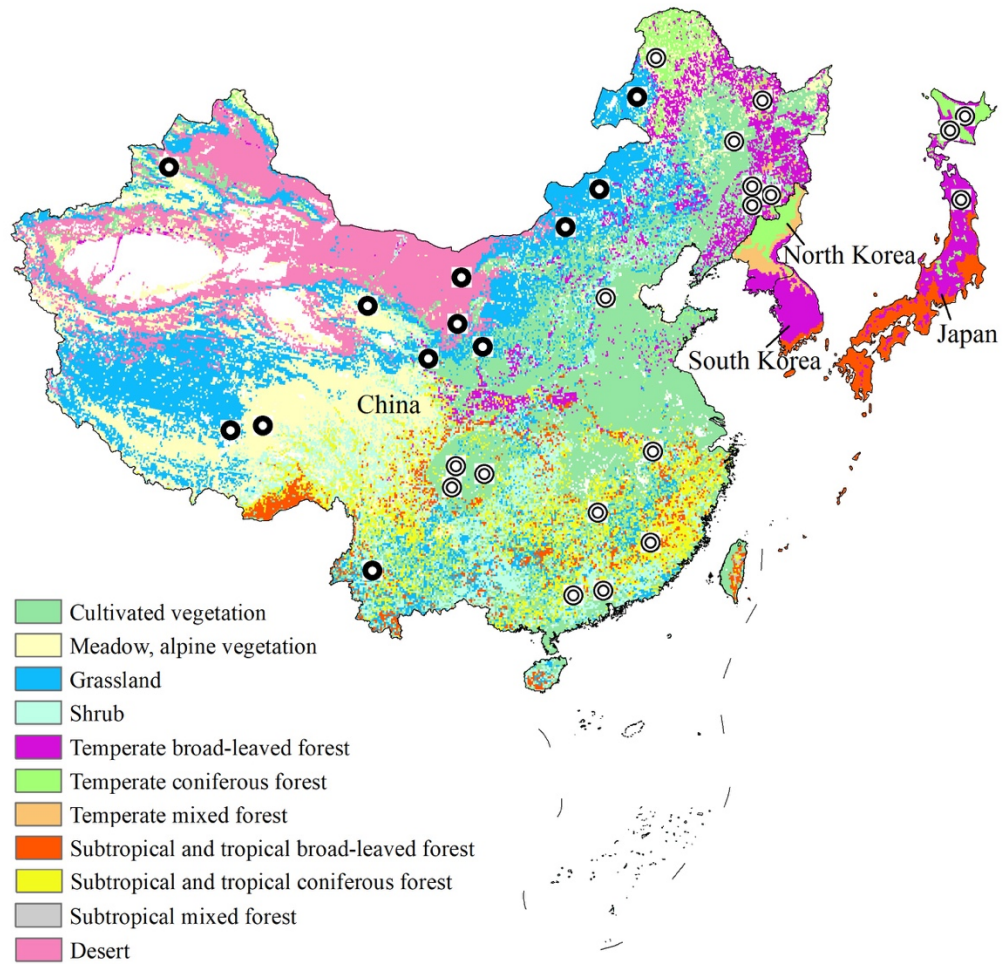


Figure 1 Vegetation map of East Asia (FAO, 2010). Some studied sites of N effects

shown as ⊙ for forests and ● for grassland.

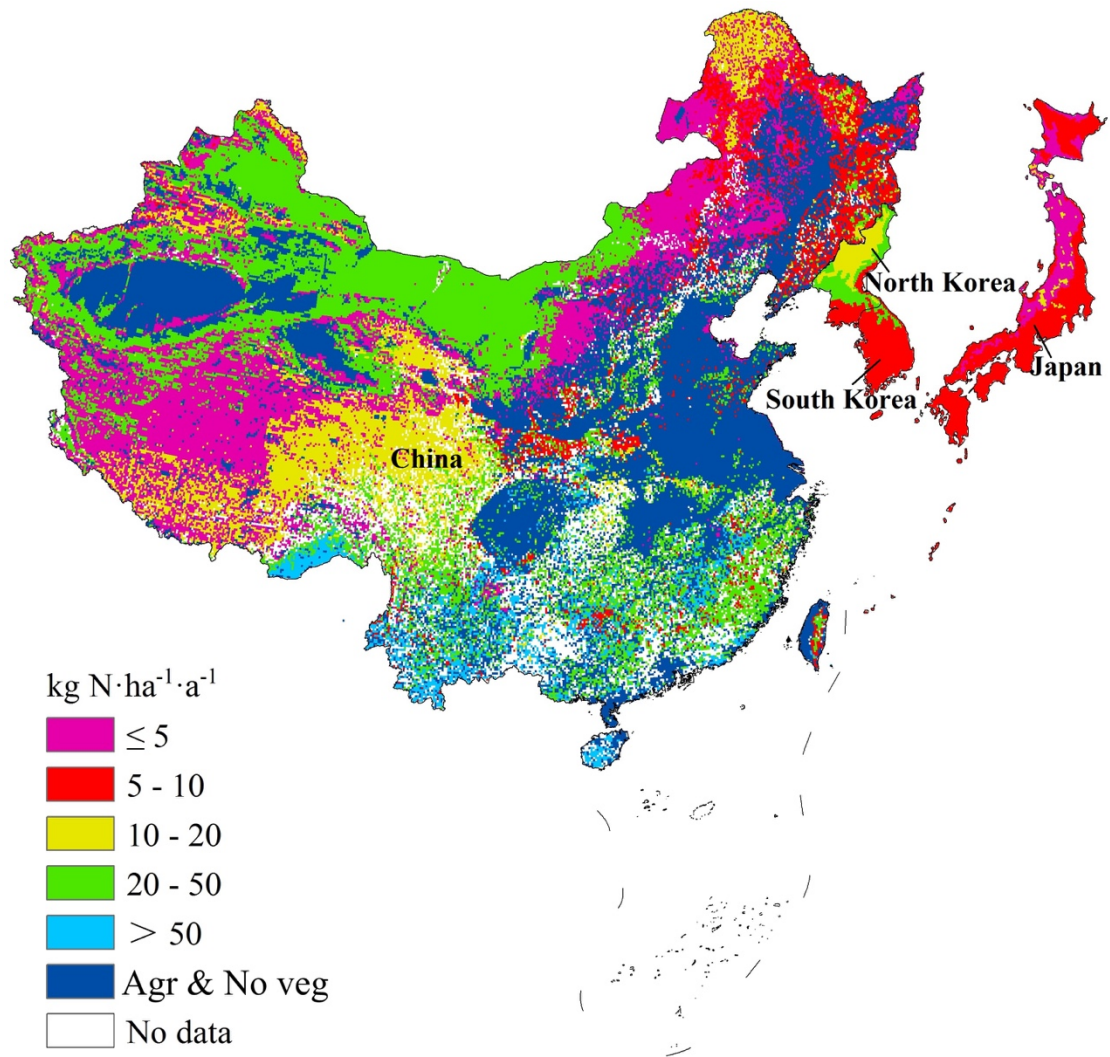


Figure 2 Empirical N critical load map based on the minimums of the critical load ranges for major forest and grassland ecosystems in East Asia. Wide-distributed agricultural fields and no vegetation regions (Agr & No veg), with theoretically very low sensitivity to N deposition and thus high critical loads, are also showed in the map.

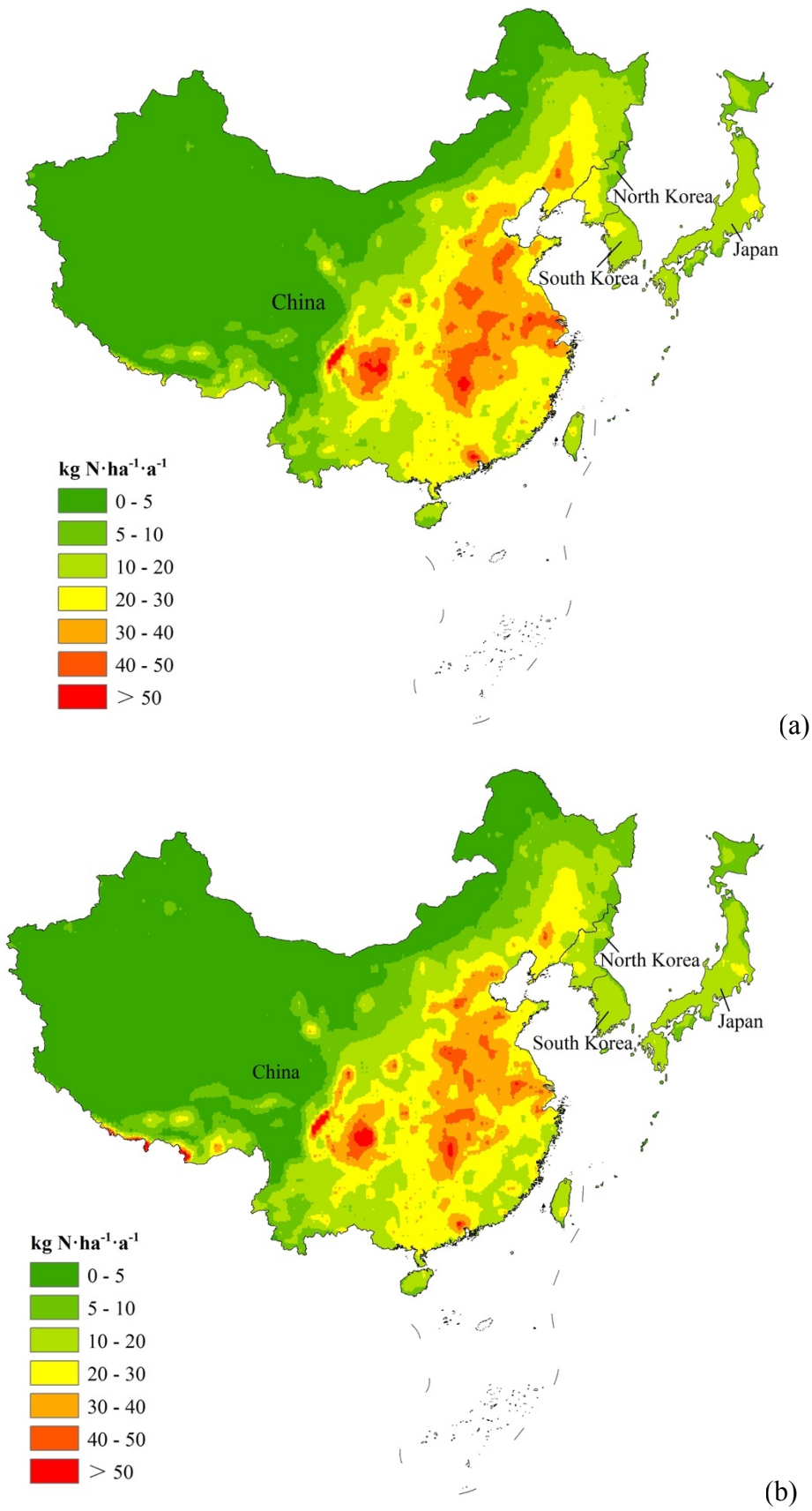


Figure 3 Modeled nitrogen deposition in (a) 2010 and (b) 2015 in East Asia.

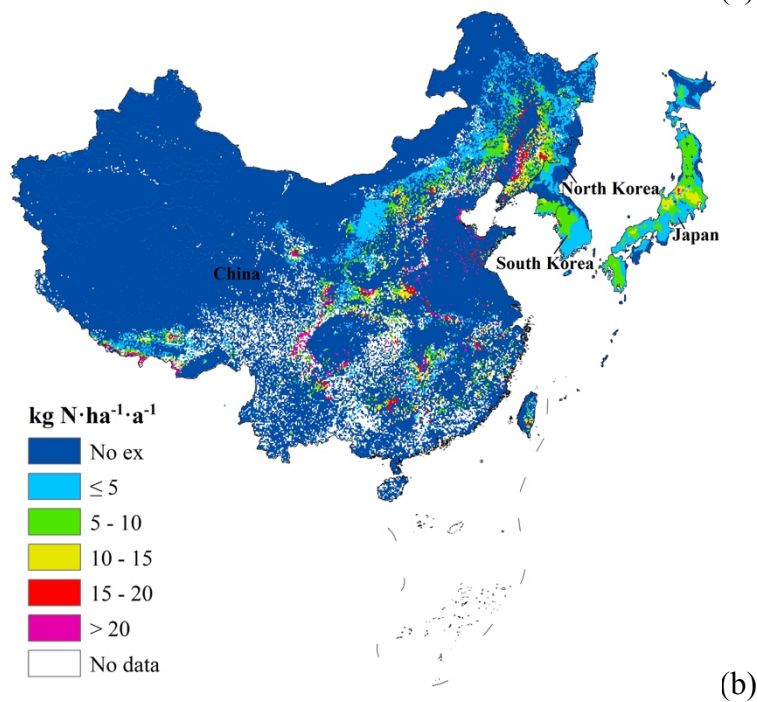
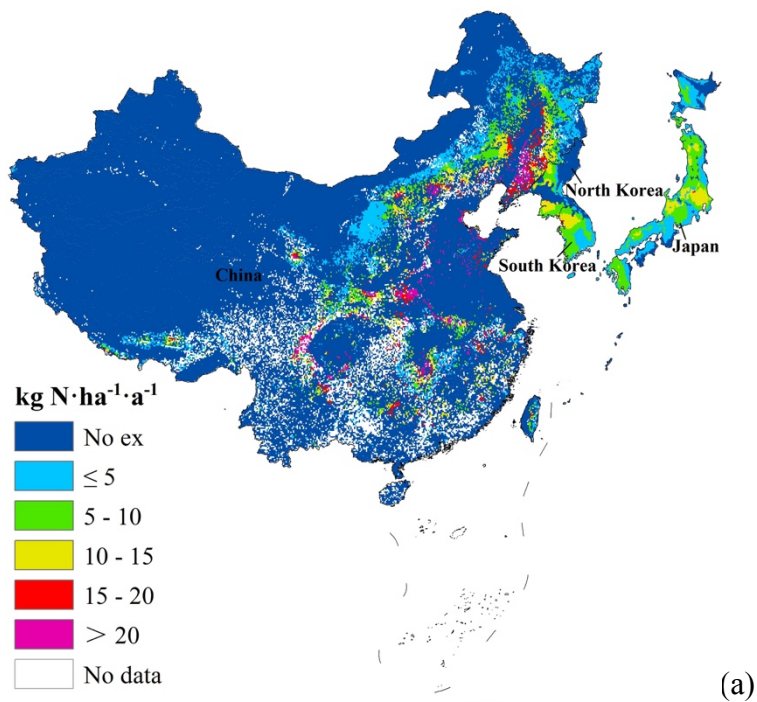


Figure 4 Critical load exceedance of nitrogen in (a) 2010 and (b) 2015 in East Asia.

Blank means no critical load data. To maximize the protection of (semi-)natural ecosystems, the minimum of critical load range for each vegetation type was used for the mapping.

Table 1 Summary of empirical critical loads of nitrogen for major forests and grasslands in East Asia*

| Vegetation | Site | Dominant specie | N deposition (kgN·ha ⁻¹ ·a ⁻¹) | N input (kgN·ha ⁻¹ ·a ⁻¹) | CL** (kgN·ha ⁻¹ ·a ⁻¹) | Duration (year) | Main response | Reference |
|---|--|--------------------------------|---|--|---|-----------------|--|---|
| FOREST | | | | | | | | |
| Subtropical coniferous plantation | Shaxian, Sanming, Fujian province, China, 117°43'E, 26°31'N | <i>Cunninghamia lanceolata</i> | 53 | 0, 60, 120, 240 | 170~300 (70~140) | 12 | Decrease in litter decomposition and needle K, Ca and Mg content; Decrease in microbial abundance and plant species richness | Fan et al., 2007ab, 2008; Liu et al., 2008; Wu et al., 2013 |
| Subtropical monsoon evergreen broad-leaved forest | Dinghushan Biosphere Reserve, Zhaoqing, Guangdong province, China, 112°33'E, 23°10'N | <i>Schima superba</i> | 38 | 0, 50, 100, 150 | 90~140 (30~70) | 16 | Change in photosynthetic and physiologic characteristics of dominant understory species; Decrease in soil microbial biomass, exchangeable base cations; Reduction in litter decomposition, DOC concentrations in soil solution and annual DOC effluxes from primary rooting zone; Decrease in soil pH and BS | Chen et al., 2012, 2013a; Fang et al., 2005, 2009; Lu et al., 2006, 2007, 2010, 2013, 2014; Mao et al., 2017; Xu et al., 2005 |
| Subtropical coniferous | Tieshanping Forest Park, Chongqing | <i>Pinus massoniana</i> | 42 | 0, 40 | 40~80 (15~30) | 15 | Increase in N leaching; Decrease | Huang et al., 2015; Lin et al., |

| | | | | | | | | |
|--|--|---|-----|------------|--------------------|----|--|--|
| forest | province, China, 106°41'E, 29°37'N | | | | | | in biomass of ground vegetation | 2007 |
| Subtropical coniferous forest | Qianyanzhou Ecological Station, Taihe city, Jiangxi Province, China, 115°03'E, 26°44'N | <i>Pinus massoniana, Cunninghamia lanceolata, Pinus elliottii</i> | 33 | 0, 40, 120 | 30~70 (15~30) | 7 | Increase in soil N ₂ O and CO ₂ emission fluxes | Li et al., 2015a |
| Subtropical evergreen broad-leaf forest | Wuyishan, Fujian province, China, 117°24'~118°02'E , 26°32'~27°55'N | <i>Castanopsis carlesii</i> | 16 | 0, 50, 100 | 70~120 (30~70) | 9 | Reduction in microbial biomass and shift of microbial community composition | Lu et al., 2014; Tian et al., 2017a |
| Subtropical evergreen broad- leaved forest | Wawushan Mountain National Forest Park, Hongya, Sichuan Province, China, 103°15'E, 29°32'N | <i>Castanopsis platyacantha, Schima sinensis</i> | 95 | 0, 50, 150 | 100~150 (30~70) | 7 | Decrease in microbial biomass C and root biomass | Peng et al., 2017 |
| Subtropical evergreen broad- leaved forest | Guniujiang, Anhui Province, China, 117°21'E, 30°01'N | <i>Castanopsis eyrei</i> | 6~7 | 0, 50, 100 | 10~60 (30~70) | 9 | Decrease in growth rate of saplings, the aboveground biomass of understory shrubs and ground-cover ferns | Tian et al., 2017b |
| Temperate coniferous forest | Changbaishan Forest Research Station, Jilin province, China, | <i>Pinus koraiensis</i> | 12 | 0, 25, 50 | 40~60 (15~30) | 13 | Decrease in soil microorganism | Zhao et al., 2008, 2009b |

| | | | | | | | | |
|---|--|---|----|-------------------------|-------------------|----|--|--|
| Temperate deciduous forest | 127°42'E, 41°41'N Fusong, Jilin province, China, 127°29'E, 42°20'N | <i>Populus alba</i> , <i>Betula platyphyl</i> | 7 | 0, 25, 50 | 10~30 (15~30) | 13 | Decrease in soil microorganism | Zhao et al., 2008, 2009b |
| Temperate deciduous forest | Lushuihe Forestry Bureau, Jilin Province, China, 128°6'E, 42°25'N | <i>Betula platyphylla</i> , <i>Populus davidiana</i> , | 25 | 0, 50 | 25~75 (10~30) | 13 | Decrease in N resorption efficiency and N use efficiency | Li et al., 2010 |
| Temperate deciduous forest | Wuyuezhai National Forest Park, Shijiazhuang, Hebei province, China, 113°52'E, 38°41'N | <i>Betula platyphylla</i> | 24 | 0, 24, 48, 96, 144, 192 | 25~120 (10~30) | 9 | Decrease in bacterial biomass and fungal biomass | Guo et al., 2017 |
| Temperate mixed broad-leaved deciduous and coniferous evergreen forests | Liangshui National Nature Reserve, Heilongjiang Province, China, 128°53'E, 47°10'N | <i>Pinus Koraiensis</i> | 13 | 0, 20, 40, 80 | 30~90 (30~50) | 5 | Increase in N ₂ O emissions | Song et al., 2017 |
| Cold-temperate and temperate mountains deciduous conifers | Maoershan Experimental Station, Heilongjiang Province, China, 127°30' ~ 127°34'E, 45°21' ~ 45°25'N | <i>Larix gmelinii</i> , <i>Fraxinus mandshurica</i> | 15 | 0, 100 | 15~115 (10~15) | 17 | Decrease in fine root biomass, soil microbial biomass, soil respiration rate, soil inorganic P availability, microbial biomass P, and acid | Hu et al., 2010; Jia et al., 2010; Yang et al., 2015, 2018 |

| | | | | | | | | |
|---|---|---|-------|------------|---------------|----|--|--|
| Cold-temperate and temperate mountains deciduous conifers | Great Xing'an Mountain, Inner Mongolia, China, 121°30'-121°31'E, 50°49'-50°51'N | <i>Larix gmelinii</i> | 10~14 | 0, 20, 40 | 30~50 (10~15) | 9 | phosphatase activity Decrease in N retention; Increase in leaching loss of NO ₃ ⁻ | Gao et al., 2016 |
| Temperate deciduous broad-leaved forest | Environmental Horticulture and Forestry Experimental Farm of Chiba University, Gunma Prefecture, central Japan, 139°00'E, 36°36'N | <i>Quercus serrata</i> , <i>Castanea crenata</i> | 3~20 | 0, 30, 150 | 5~170 | 8 | Increase in N ₂ O emissions | Kong et al., 2013 |
| Temperate coniferous forest | Sapporo Experimental Forest of Hokkaido University, Japan, 141°20'E, 43°06'N | <i>Larix kaempferi</i> | 3~20 | 0, 50 | 5~70 | 11 | Increase in N ₂ O emissions; Decrease in ECM diversity and community structure | Kim et al., 2012; Wang et al., 2018 |
| Temperate deciduous broad-leaved forest | Tomakomai Experimental Forest, Hokkaido University, northern Japan, 141°36'E, 42°40'N | <i>Quercus crispula</i> | 3~20 | 0, 100 | 5~120 | 3 | Decrease in diversity index | Lee et al., 2017 |

Table 1 (Continued)

| Vegetation | Site | Dominant specie | N dep (kgN·ha ⁻¹ ·a ⁻¹) | N input (kgN·ha ⁻¹ ·a ⁻¹) | CL** (kgN·ha ⁻¹ ·a ⁻¹) | Duration (year) | Main response | Reference |
|--------------------------------------|--|---|---|---|--|--------------------|---|---|
| GRASSLAND | | | | | | | | |
| Temperate needlegrass arid steppe | Inner Mongolia Grassland Ecosystem Research Station (IMGERS), Xilin River Basin, Inner Mengonia, 116°40'E, 43°32'N | <i>Leymus chinensis</i> | 4 | 0, 17.5, 52.5, 105, 175, 280 | 110~180 for degraded; 30~50 for natural (15~30) | 19 | Peak value reached for specific leaf area, leaf N content, and total chlorophyll content; Reduction in richness of plant species and biomass of perennial bunch grass | Bai et al., 2009; Chen et al., 2013b; Lan and Bai, 2012; Li et al., 2015b; Pan et al., 2004, 2005; Qin et al., 2011; Song et al., 2011; Tian et al., 2016; Wan et al., 2008; Wei et al., 2014 Xu et al., 2017 |
| Temperate needlegrass arid steppe | Duolun, Inner Mongolia, 116°17'E, 42°02'N | <i>Agropyron cristatum</i> , <i>Artemisia scoparia</i> | 4 | 0, 50, 100, 150 | 55~155 (15~30) | 14 | Reduction in belowground net primary production | |
| Temperate needlegrass arid steppe | Taibus Banner, Inner Mongolia Autonomous Region of China, Inner Mongolia, 115°29'E, 42°06'N | <i>Stipa krylovii</i> , <i>Artemisia frigida</i> | 35 | 0, 20, 50, 100, 200, 500 | 50~85 (15~30) | 5 | Reduction in species richness | He et al., 2016 |
| Temperate needlegrass arid steppe | Yunwushan Grassland Natural Reserve, Ningxia, 105°20'-106°58'E, 35°14'-36°38'N | <i>Thymus mongolicus</i> | 3 | 0, 50, 100 | 50~100 (15~30) | 3 | <i>Thymus mongolicus</i> community replaced by <i>Stipa hungeana</i> | Cheng et al., 1996 |
| Subtropical and tropical grass- forb | Dongchuan Mudflow Monitoring | <i>Heteropogon Contortus</i> | 4 | 0, 50, 150, 250 | 150~250 (30~70) | 1 | <i>Gramineae</i> dominant | Zhang et al., 2004 |

| | | | | | | | | | |
|---------------|--|-------------------------|------|------------------------|---------------|----|---|---------------------------------------|--|
| community | Station, Xiaojiang River Basin, Yunan, 103°E, 26°N | | | | | | | | |
| Alpine meadow | Nagqu County, Nagqu Prefecture, Tibet Autonomous Region, 92.017°E, 31.441°N | <i>Kobresia pygmaea</i> | 7 | 0, 7, 20, 40 | 15~50 (15~30) | 5 | Increase in N ₂ O emission | Yan et al., 2018 | |
| Alpine meadow | Haibei alpine meadow ecosystem research station, Chinese Academy of Sciences, 101°19'E, 37°37'N | <i>Kobresia humilis</i> | 4~14 | 0, 10, 20, 40 | 25~35 (15~30) | 12 | Decrease in soil pH and CH ₄ uptake | Fang et al., 2014; Jiang et al., 2010 | |
| Alpine steppe | Nam Co Monitoring and Research Station for Multisphere Interactions, Chinese Academy of Sciences, 90°58'E, 30°47'N | <i>Kobresia pygmaea</i> | 7 | 0, 10, 20, 40, 80, 160 | 20~50 (15~30) | 9 | Reduction in biomass N:P ratios, N-uptake efficiency and N-use efficiency | Liu et al., 2013b | |
| Alpine steppe | Bayinbuluk Grassland Ecosystem Research Station, Chinese Academy of Sciences, southern Tianshan mountains, Xinjiang Uygur Autonomous | <i>Stipa purpurea</i> | 5 | 0, 10, 30, 90, 150 | 5~15 (15~30) | 3 | Increase N ₂ O emission | Li et al., 2012a,b | |

| | | | | | | | | |
|--------------------------------|--|-------------------------------|----|----------------|---------------|----|---|--------------------|
| Temperate grass-forb Community | Region, 83°42.5'E, 42°53.1'N State Key Laboratory of Soil Erosion and Dryland Farming on the Loess plateau in Yangling, Shanxi province, 108°7'E, 34°27'N | <i>Bothriochloa ischaemum</i> | 2 | 0, 25, 50, 100 | 5~30 (15~30) | 6 | Reduction in microbial community and microbial diversity | Zhang et al., 2017 |
| Temperate grass-forb meadow | Inner Mongolia Grassland Ecosystem Research Station, Hulunbuir, Inner Mongolia 119°55'-119°58'E, 49°19'-49°21'N | <i>Stipa baicalensis</i> | 10 | 0, 10, 20 | 10~30 (10~15) | 11 | Increase in N ₂ O emission; Decrease in CH ₄ uptake | Liu et al., 2017b |

* This table was updated from the reviews by Liu et al. (2011) and Duan et al. (2014). Many results published after 2010 were added.

** Values in bracket are critical loads of nutrient N calculated by the steady state mass balance (SSMB) method (Duan et al., 2001; Zhao et al., 2009a).

Table 2 Area and total amount of the critical load exceedance in East Asia

| Year | Area (Mha)* | | | | Total amount (Mt N·a ⁻¹) | | | |
|------|-----------------|------------------|-----------------|----------------|--------------------------------------|------------------|-------|-------|
| | China | Korean peninsula | Japan | Total | China | Korean peninsula | Japan | Total |
| 2010 | 105 (10.9%) | 13.9 (62.5%) | 30.8 (81.4%) | 150 (14.6%) | 11.6 | 0.37 | 0.50 | 12.5 |
| 2015 | 99.1 (10.3%) | 13.9 (62.5%) | 28.7 (75.8%) | 142 (13.8%) | 11.1 | 0.32 | 0.47 | 11.9 |

* The figures in parentheses means ratio of the area of critical load exceedance to the land area.